BIOCHEMISTRY
including biophysical chemistry & molecular biology

Article

pubs.acs.org/biochemistry

Structural Basis for the Interaction between Pyk2-FAT Domain and Leupaxin LD Repeats

Murugendra S. Vanarotti,[†] David B. Finkelstein,[‡] Cristina D. Guibao,[†] Amanda Nourse,[†] Darcie J. Miller,[*,†] and Jie J. Zheng[*,†,§]

[†]Department of Structural Biology and [‡]Hartwell Center for Bioinformatics and Biotechnology, St. Jude Children's Research Hospital, Memphis, Tennessee 38105, United States

[§]Stein Eye Institute, Department of Ophthalmology, David Geffen School of Medicine at UCLA, Los Angeles, California 90095, United States

Supporting Information

ABSTRACT: Proline-rich tyrosine kinase 2 (Pyk2) is a nonreceptor tyrosine kinase and belongs to the focal adhesion kinase (FAK) family. Like FAK, the C-terminal focal adhesion-targeting (FAT) domain of Pyk2 binds to paxillin, a scaffold protein in focal adhesions; however, the interaction between the FAT domain of Pyk2 and paxillin is dynamic and unstable. Leupaxin is another member in the paxillin family and was suggested to be the native binding partner of Pyk2; Pyk2 gene expression is strongly correlated with that of leupaxin in many tissues including primary breast cancer. Here, we report that leupaxin interacts with Pyk2-FAT. Leupaxin has four leucine−aspartate (LD) motifs. The first and third LD motifs of leupaxin preferably target the two LD-binding sites on the Pyk2-FAT domain, respectively. Moreover, the full-length leupaxin binds to Pyk2-FAT as a stable one-to-one complex. Together, we propose that there is an underlying selectivity between leupaxin and paxillin for Pyk2, which may influence the differing behavior of the two proteins at focal adhesion sites.

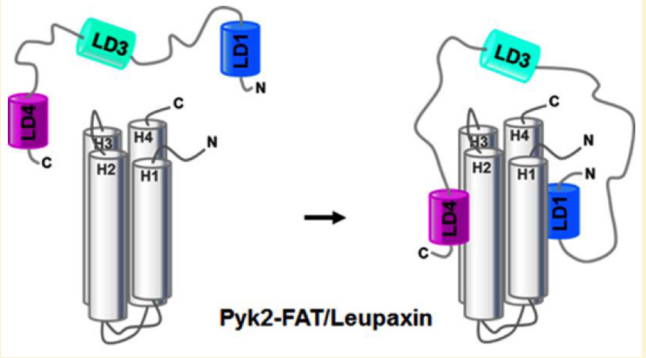

Proline-rich tyrosine kinase 2 (Pyk2) is a nonreceptor tyrosine kinase that belongs to the focal adhesion kinase (FAK) family.[1−4] Recently, several studies have demonstrated that Pyk2 is highly expressed in a variety of human tumors and may serve as a novel biomarker with prognostic significance in neuroglioma, breast cancer, and hepatocellular carcinoma.[1,5−8] FAK family proteins have a large N-terminal FERM domain, a centrally located kinase domain, and a C-terminal focal adhesion targeting (FAT) domain.[9] Despite the structural similarities between FAK and Pyk2 kinases, FAK is ubiquitously expressed, whereas Pyk2 shows more tissue-specific expression.[1,3,10−12] Pyk2 is highly expressed in endothelium, central nervous system, and hematopoietic lineages.[13−16] Previous studies in several cell types have shown that expression of endogenous Pyk2 was observed when FAK levels are low,[17−19] suggesting that a compensatory role of Pyk2 can be acquired by cells to maintain the regulatory function of FAK during cell adhesion and migration. However, FAK does not compensate for Pyk2 in Pyk2-deficient B cells and macrophages.[20] Therefore, it appears that FAK and Pyk2 differ from each other in regulating cellular functions and signaling pathways.

The FAT domain of FAK binds to paxillin, a major scaffold protein in focal adhesions;[21−25] this interaction is required to recruit FAK to form robust focal adhesions.[26] The C-terminal half of paxillin has four well-folded LIM domains that are used to target focal adhesions. The N-terminal region is generally disordered in the apo state and contains four or five LD motifs linked by unstructured loops in a "beads on a string" fashion. These LD motifs interact with other FA proteins, including the FAT domain of FAK and Pyk2.[22] We[27] and others[28−32] have determined the structure of the FAT domain of FAK by NMR and X-ray crystallography studies. The structure of the FAT domain is a four-helix bundle. Two potential LD peptide binding sites were found on the surface of the FAT domain: one spanning helices H1 and H4 (H1/H4 site) and one spanning helices H2 and H3 (H2/H3 site).[27−30] By conducting a detailed, systematic study using NMR and other biophysical approaches, we showed that the LD2 and LD4 motifs of a paxillin molecule bind simultaneously to a single FAT domain; the LD2 motif binds at the H1/H4 site and the LD4 motif binds at the H2/H3 site.[33]

Like FAK, Pyk2 also has a C-terminal FAT domain that forms a four-helix bundle (H1−H4).[28,33−36] However, our recent studies showed that the binding mechanism between Pyk2 and FAK for paxillin LD2 and LD4 motifs is different; in Pyk2, paxillin LD2 and LD4 motifs compete equally for the

Received: November 24, 2015
Revised: February 11, 2016
Published: February 11, 2016

DOI: 10.1021/acs.biochem.5b01274
Biochemistry 2016, 55, 1332−1345

high-affinity binding site H2/H3 and undergo a conformational switching mechanism.[36] In other words, paxillin forms a much more stable complex with the FAT domain of FAK than with the FAT domain of Pyk2. Indeed, paxillin binds more tightly to the FAT domain of FAK than the FAT domain of Pyk2. Such observation led us to speculate that paxillin is not the native binding partner of Pyk2 and that the FAT domain of Pyk2 should form a stable complex with its native binding partner.

Leupaxin was initially identified as a leukocyte-specific isoform of paxillin[37] and shares the highest sequence similarity with paxillin of any paxillin family member. It is preferentially expressed in macrophages, osteoclasts, and hematopoietic cells.[37,38] Previous studies have demonstrated that Pyk2 associates with leupaxin in lymphoid cells, where these proteins may form a cell type-specific signaling complex.[38] Furthermore, the association of these two proteins can modulate cell migration, adhesion, and motility in prostate cancer.[38] Like paxillin, leupaxin is composed of multiple functional modules, including leucine−aspartate (LD) motifs and LIM domains, suggesting that leupaxin also serves as a molecular adaptor at focal adhesions. Phylogenetic tree and sequence analysis suggest that, unlike paxillin, leupaxin has four LD repeats (LD1, LD3, LD4, and LD5) at its N-terminus.[39] Leupaxin does not contain an equivalent paxillin LD2 motif. Hence, it has been speculated that in the absence of the LD2 motif a potential interaction between leupaxin and FAK would be relatively weak.[37]

In this study, we examined the interaction between leupaxin and Pyk2. We determined how the LD motifs of leupaxin bind to Pyk2-FAT using various biophysical methods, including isothermal titration calorimetry (ITC) and nuclear magnetic resonance (NMR). We also present two crystal structures of Pyk2-FAT complexes with high-affinity leupaxin LD1 and LD4 peptides and its stable 1:1 interaction with full-length leupaxin. Considering our studies along with previous reports, we identify an underlying selectivity difference between leupaxin and paxillin in the way they associate with Pyk2 that directly affects their complex stability and may ultimately influence the behavior of Pyk2 at focal adhesion sites.

EXPERIMENTAL PROCEDURES

Analysis of GEO Profiling. Publically available data sets that assayed breast cancer primary tumors (GSE1276) and normal breast cells (GSE20437) were downloaded.[40] MAS 5.0 signal data was log start transformed by the following formula: $\log_2$(signal + 20); it was then plotted and correlated. Data transformations, scatterplots, linear fits, and Pearson correlations were generated using STATA/MP 11.2. Typically, a correlation sums the gene expression differences between any two genes across multiple arrays and then divides that sum by the total number of array experiments examined to give the Pearson's ρ. ρ values, which measure the degree of association between variables, range from −1 to 1.

Cloning, Expression, and Purification of the FAT Domain of Pyk2. The FAT domain of human Pyk2 (residues 871−1005) was expressed as an N-terminal His-tag fusion in *Escherichia coli* cells and purified as described.[36] The Pyk2-FAT protein concentration was measured using a standard Coomassie (Bradford) protein assay. The final protein buffer used for all NMR experiments, biochemical studies, and X-ray crystallization was 20 mM MES, pH 6.2.

Cloning, Expression, and Purification of Leupaxin$^{1-105}$. The coding sequence of leupaxin$^{1-105}$ (human leupaxin, residues 1−105; Figure S13A) was cloned into the pET-28 expression vector (Novagen). Protein was then expressed as an N-terminal His-tag fusion in *E. coli* Rosetta2 (DE3) pLysS cells (Novagen). Cells were initially grown at 37 °C and induced with 1 mM IPTG at 18 °C overnight. Protein was purified using nickel-column affinity chromatography followed by HPLC (Figure S13B,C). To avoid nonspecific proteolysis by thrombin, the N-terminal His-tag was not cleaved during purification. The ^{15}N-labeled and ^{13}C/^{15}N-labeled samples were prepared by growing the cells in MOPS-buffered media containing $^{15}NH_4Cl$ (1 g/L) and [^{13}C6]glucose (3 g/L).[41] All biochemical and structural studies of leupaxin$^{1-105}$ were performed in 20 mM MES buffer, pH 6.2.

Cloning, Expression, and Purification of Leupaxin$^{1-151}$. The coding sequence of leupaxin$^{1-151}$ (human leupaxin, residues 1−151) was cloned into the pET-28 expression vector (Novagen). The expression and purification procedure of the leupaxin$^{1-151}$ construct was similar to those for the leupaxin$^{1-105}$ construct.

Cloning, Expression, and Purification of Pyk2-FAT-LD1 Constructs. Pyk2-FAT-LD1 fusion constructs were generated using Pyk2-FAT as a template. Double-stranded DNA corresponding to the "GGS-LD1" sequence (CCTGCAGGGGGCGGCATGGAGGAACTGGATGCGTTACTGGAAGAACTGGAACGTAGCACCTTACAGGATAGCGATTAG) was obtained from Integrated DNA Technologies and cloned using the *Pst*I restriction enzyme site downstream of the existing Pyk2-FAT construct in the pET28a vector. Site-directed mutagenesis was performed to remove the stop codon at the end of the Pyk2-FAT sequence and to add additional residues. The expression and purification procedures for Pyk2-FAT-LD1 were similar to those for the Pyk2-FAT construct.

Synthesis of Leupaxin Peptide Mimics LD1, LD3, LD4, and LD5. Leupaxin derived peptides leupaxin-LD1 (human leupaxin, residues 1−20), leupaxin-LD3 (human leupaxin, residues 36−56), leupaxin-LD4 (human leupaxin, residues 86−104), and leupaxin-LD5 (human leupaxin, residues 125−150) were chemically synthesized and purified by high-pressure liquid chromatography (HPLC) at the Hartwell Center of Bioinformatics and Biotechnology of St. Jude Children's Research Hospital. The length of the leupaxin-LD1, leupaxin-LD3, leupaxin-LD4, and leupaxin-LD5 peptides used was based on our previous paxillin binding studies with Pyk2,[36] FAK,[27] and GIT1.[42] All peptide stocks were prepared at a concentration of 5 mM in 20 mM MES, pH 6.2.

Isothermal Titration Calorimetry (ITC). ITC experiments were performed using a Microcal ITC200 instrument (Microcal). Sample buffer conditions for ITC studies were the same as those for NMR studies. The sample cell of the calorimeter was loaded with 100 μM Pyk2-FAT in 20 mM MES, pH 6.2. The syringe was loaded with leupaxin-LD1, leupaxin-LD3, leupaxin-LD4, and leupaxin-LD5 peptides and leupaxin$^{1-105}$ (1000 μM leupaxin-LD1, leupaxin-LD3, leupaxin-LD4, or leupaxin-LD5; 500 μM leupaxin$^{1-105}$) for titrations in the same buffer. All solutions were degassed for 10 min. For leupaxin-LD3, leupaxin-LD5, and leupaxin$^{1-105}$ binding to Pyk2-FAT, titrations were performed at 25 °C with injection volumes of 2 μL and a spacing of 120 s. However, for leupaxin-LD1 and leupaxin-LD4 binding to Pyk2-FAT, titrations were performed at 15 °C with injection volumes of 2 μL and a spacing of 120 s. These low temperature experiments for the leupaxin-LD1 and leupaxin-LD4 peptides were performed to observe the second weak binding site by ITC, which we could not achieve when

DOI: 10.1021/acs.biochem.5b01274
Biochemistry 2016, 55, 1332−1345

Table 1. Thermodynamic Parameters for the Binding of Pyk2-FAT to Leupaxin LD1, LD3, LD4, and LD5 Peptides and Leupaxin$^{1-105}$ Obtained by ITC

	sites (n)	K_D (μM)	ΔG (kcal/mol)	ΔH (kcal/mol)	$-T\Delta S$ (kcal/mol)
LD1[a]	first	2.8 ± 1.0	−7.6 ± 0.3	−2.0 ± 0.2	−5.6 ± 0.4
	second	52.0 ± 26.0	−5.3 ± 0.7	1.6 ± 0.3	−7.0 ± 0.5
LD3[a,b]					
LD4[a]	first	2.2 ± 1.0	−7.6 ± 0.3	−3.0 ± 0.2	−4.6 ± 0.6
	second	33.0 ± 7.2	−6.0 ± 0.1	0.5 ± 0.3	−6.5 ± 0.4
LD5[a,b]					
leupaxin$^{1-105}$	1.0	0.6 ± 0.2	5.9 ± 0.2	−2.5 ± 0.5	−3.4 ± 0.05

[a]The peptide sequences are shown in Figure S3A. [b]Not Determined.

experiments were performed at 25 °C. Control experiments were performed by injecting leupaxin-LD1, leupaxin-LD3, leupaxin-LD4, or leupaxin-LD5 peptide and leupaxin$^{1-105}$ into the buffer solution in an identical manner, and the resulting heat changes were subtracted from the measured heats of binding. The data were fit using a one-site binding model and two-site sequential binding model available in Origin ITC data analysis software (v. 7.0). All ITC experiments were performed in duplicate. The results are shown in Table 1.

Crystallization, Structure Determination, and Model Quality. For all crystallographic analyses, model building was performed using Coot,[43] minimization, ADP, and TLS refinement were performed in Phenix,[44] and 5% of the data was sequestered for the calculation of R_{free}. Additionally, final structure statistics were calculated using MolProbity,[45] and structural figures were generated with PyMOL.[46]

Pyk2-FAT/Leupaxin-LD1 Complex Structure. The FAT domain of Pyk2 was cocrystallized with leupaxin-LD1 peptide by sitting-drop vapor diffusion at 18 °C. The 400 nL drop contained 200 nL of protein/leupaxin-LD1 peptide mixture (20 mM MES, pH 6.2, 0.5 mM protein, and 2 mM peptide) and 200 nL of well solution (100 mM Tris, pH 8.5, 0.2 M $MgCl_2$, and 30% (w/v) PEG 4000). The crystals were cryo-preserved in 20% (v/v) glycerol/80% (v/v) well solution. Native data were collected at Southeast Regional Collaborative Access Team (SER-CAT) beamline 22-BM. Data were integrated and scaled to 2.5 Å using HKL2000.[47]

The 2.5 Å crystal structure of Pyk2-FAT (3GM3) served as the Phaser molecular replacement model.[48] The crystals belong to space group $P2_12_12_1$ with two 1:2 Pyk2-FAT/leupaxin-LD1 complexes in the asymmetric unit. The two complexes include chains A/B/C and D/E/F, where chains A and D correspond to Pyk2-FAT, chains B and E correspond to leupaxin-LD1 bound at H1/H4, and chains C and F correspond to leupaxin-LD1 bound at the H2/H3 site. Although the two complexes in the asymmetric unit are very similar, detailed descriptions are provided for complex ABC only; electron density for protein/peptide interactions in ABC is of relatively higher quality, allowing for a more complete description of key interactions. In addition, the peptides for this complex are solvent-exposed and not stabilized or perturbed by crystal packing. Leupaxin-LD1 peptide final simulated annealing omit maps are provided in Figure 2A,C. Ramachandran statistics show that 98.1 and 1.9% of the residues are in the preferred and allowed regions, respectively.

Pyk2-FAT/LD4 Complex Structure. Pyk2-FAT was cocrystallized with leupaxin-LD4 peptide by sitting-drop vapor diffusion at 18 °C. The 4 μL drop contained 2 μL of protein/LD4 peptide mixture (20 mM MES, pH 6.2, 0.5 mM protein, and 2 mM peptide) and 2 μL of well solution (100 mM Tris, pH 9.0, and 45% (v/v) PEG 600). Native data were collected at SER-CAT beamline 22-ID. Data were integrated and scaled to 1.8 Å using HKL2000.[47]

Molecular replacement proceeded as described for Pyk2-FAT/leupaxin-LD1. The crystals belong to space group $P2_12_12$ with one 1:1 complex of Pyk2-FAT/leupaxin-LD4 (complex A/C) in the asymmetric unit. Peptide chain C binds at the 2/3 site. The 1/4 site was blocked by crystal packing. Leupaxin-LD4 peptide final simulated annealing omit map is provided in Figure 3A. Ramachandran statistics show that 99.3 and 0.7% of the residues are in the preferred and allowed regions, respectively.

Pyk2-FAT-LD1/Leupaxin-LD4 Complex Structure. Pyk2-FAT-LD1 fusion protein was cocrystallized with leupaxin-LD4 peptide by sitting-drop vapor diffusion at 18 °C. The 4 μL drop contained 2 μL of protein/leupaxin-LD4 peptide mixture (20 mM MES, pH 6.2, 0.5 mM protein, and 2 mM peptide) and 2 μL of well solution (100 mM MES, pH 6.5, and 25% (w/v) PEG 3000). Native data were collected at SER-CAT beamline 22-BM. Data were integrated and scaled to 2.0 Å using XDS.[49]

Molecular replacement proceeded as described for Pyk2-FAT/leupaxin-LD1. The crystals belong to space group $P2_1$ with two 1:1 Pyk2-FAT-LD1/leupaxin-LD4 complexes in the asymmetric unit. The two complexes include chains A/C and D/F, where chains A and D correspond to the Pyk2-FAT-LD1 fusion protein and chains C and F correspond to leupaxin-LD4 bound at the H2/H3 site. Final simulated annealing omit maps are provided in Figures 7B and S11A. Ramachandran statistics show that 99.4 and 0.6% of the residues are in the preferred and allowed regions, respectively.

Size-Exclusion Chromatography Multiangle Light Scattering (SEC-MALS). Pyk2-FAT/leupaxin$^{1-151}$ was analyzed by size-exclusion chromatography (Shodex KW-802.5) coupled to in-line multi-angle light scattering (SEC-MALS) (Wyatt DAWN HELEOS) with in-line refractive index detection (Wyatt Optilab rEX). The wavelength used was 658 nm, and the calibration constant was 2.32950×10^{-4} 1/(V cm). The column was equilibrated with 20 mM MES, pH 6.2, 50 mM NaCl, and experiments were conducted at 25 °C. The injected sample volume was 30 μL, and experiments were conducted at a flow rate of 0.5 mL/min. The size-exclusion limit of the column was 60 kDa, and protein was loaded at 0.19 mg/mL. Eluted protein was detected via light scattering and refractive index, and data were recorded and analyzed with Wyatt Astra software (version 6.1). The refractive index increment, dn/dc, was assumed to be 0.185 mL/g.

NMR Spectroscopy and Chemical Shift Perturbation (CSP) Analysis. All NMR experiments were collected at 600 and 800 MHz on $^{13}C/^{15}N$- and ^{15}N-labeled samples of Pyk2-

DOI: 10.1021/acs.biochem.5b01274
Biochemistry 2016, 55, 1332−1345

Table 2. Data Collection and Refinement Statistics[a]

	Pyk2-FAT/leupaxin-LD1	Pyk2-FAT/leupaxin-LD4	Pyk2-FAT-LD1/leupaxin-LD4
Data Collection			
space group	$P2_12_12_1$	$P2_12_12$	$P2_1$
Cell Dimensions			
a, *b*, *c* (Å)	27.5, 78.1, 165.4	138.0, 30.5, 40.6	52.1, 79.2, 53.2
α, β, γ (deg)	90.0, 90.0, 90.0	90.0, 90.0, 90.0	90.0, 117.6, 90.0
resolution (Å)	2.5 (2.59−2.50)[b]	1.8 (1.86−1.80)	2.0 (2.12−2.0)
R_{sym} (%)	9.0 (55.6)	5.0 (36.8)	3.9 (42.8)
$I/\sigma I$	20.9 (2.2)	46.9 (3.5)	18.6 (2.4)
completeness (%)	98.4 (91.7)	95.9 (76.2)	95.5 (77.3)
redundancy	7.5 (5.0)	8.9 (6.7)	4.2 (3.2)
Refinement			
resolution (Å)	25.0−2.5	35.0−1.8	30.0−2.0
no. reflections	12 885	16 103	24 569
R_{work}/R_{free}	22.4/26.6	20.8/23.1	20.4/25.0
No. Atoms			
protein	2045	1039	2247
peptide	385	106	261
water	12	67	71
B-factors			
protein	48.5	38.4	58.9
peptide	66.7	46.0	78.5
water	46.2	39.2	53.5
RMS Deviations			
bond lengths (Å)	0.009	0.007	0.007
bond angles (deg)	1.1	0.9	1.0

[a]Each data set was collected from a single crystal. [b]Values in parentheses are for the highest resolution shell.

FAT and leupaxin$^{1-105}$ at 305 K. NMR spectra were then processed with Topspin 3.1 and analyzed using CARA 1.8.4.[50] All experiments of Pyk2-FAT and leupaxin$^{1-105}$ were carried out in 20 mM MES, pH 6.2, at a molar concentration of 200 μM. Leupaxin-LD1, leupaxin-LD3, leupaxin-LD4, and leupaxin-LD5 peptide stocks were prepared in the Pyk2-FAT dialysis buffer, and their pH was readjusted to 6.2 before titration. Backbone assignments of Pyk2-FAT, Pyk2-FAT-LD1, and leupaxin$^{1-105}$ were obtained based on HNCACB, CBCA(CO)-NH, HNCA, and HN(CO)CA experiments.

For CSP analysis, NMR titration of leupaxin-LD1 and leupaxin-LD4 peptides to Pyk2-FAT was performed by adding the following protein/peptide ratios: 1:0.4, 1:0.8, 1:1.2, 1:1.6, 1:2.4, and 1:4. Pyk2-FAT titration to leupaxin$^{1-105}$ was also performed by adding similar ratios. NMR titration of leupaxin-LD1 and leupaxin-LD4 peptides to Pyk2-FAT-LD1 was performed by adding the following protein/peptide ratios: 1:0.4, 1:0.8, 1:1.2, 1:1.6, and 1:2. Similarly, a leupaxin-LD1 and leupaxin-LD4 peptide mixture (1:1) was titrated to ^{15}N-labeled Pyk2-FAT by adding the following protein/peptide ratios: 1:0, 1:0.4, 1:0.8, 1:1.2, 1:1.6, and 1:2. A series of ^{1}H−^{15}N-HSQC and ^{1}H−^{15}N-TROSY spectra were collected on Bruker 600 and 800 MHz spectrometers, and data was analyzed using CARA 1.8.4. ^{15}N and ^{1}H chemical shift values for the displaced peaks in ^{1}H−^{15}N-HSQC and ^{1}H−^{15}N-TROSY titration experiments were determined for each of the successive titration points using CARA. To determine the per-residue chemical shift perturbation upon binding and account for differences in spectral widths between ^{15}N and ^{1}H resonances,[51] weighted average chemical shift differences, Δav(HN) were calculated for the backbone amide ^{1}H and ^{15}N resonances using the following equation: Δav(NH) = [(ΔH2+ (ΔN/5)2)/2]1/2, where ΔH and ΔN are chemical-shift differences for ^{1}H and ^{15}N, respectively.[20,52,53]

RESULTS

Pyk2 Gene Expression Profile. It was shown that both Pyk2 and leupaxin exhibit elevated expression levels in prostate cancer, where they associate and affect cell adhesion and migration.[37,38] We questioned whether such a correlation might also be found in other systems. Because it is also known that Pyk2 is highly expressed in breast cancer cells,[54] we therefore investigated whether this elevated Pyk2 gene expression similarly correlates with leupaxin in breast cancer as well. We decided to analyze the Pyk2 gene expression profiles of primary breast tumor and normal breast cells using the GEO database.[40] We downloaded raw data from primary breast tumors (GSE1276) and normal breast cells (GSE20437). Pearson correlations of Pyk2 with paxillin and leupaxin were examined and compared with those of FAK. In normal breast cells, we found that leupaxin negatively correlated with Pyk2 gene expression (ρ = −0.44), consistent with the notion that leupaxin is not preferentially expressed in these cells. In primary breast tumors, we found that Pyk2 expression correlated more strongly with leupaxin than paxillin, with ρ values of 0.46 and 0.20, respectively (Figure S1). Moreover, we detected a negative Pearson correlation for FAK expression with leupaxin (ρ = −0.09) and a positive correlation for paxillin (ρ = 0.52) in primary breast cancer cells. These results suggest that Pyk2 gene expression is correlated with leupaxin and that FAK gene expression is correlated with paxillin in primary breast cancer tumors. Such tight correlations among the four proteins is in agreement with the notion that paxillin is the native binding partner of FAK and that leupaxin is the native binding partner of Pyk2.[37,55]

DOI: 10.1021/acs.biochem.5b01274
Biochemistry 2016, 55, 1332−1345

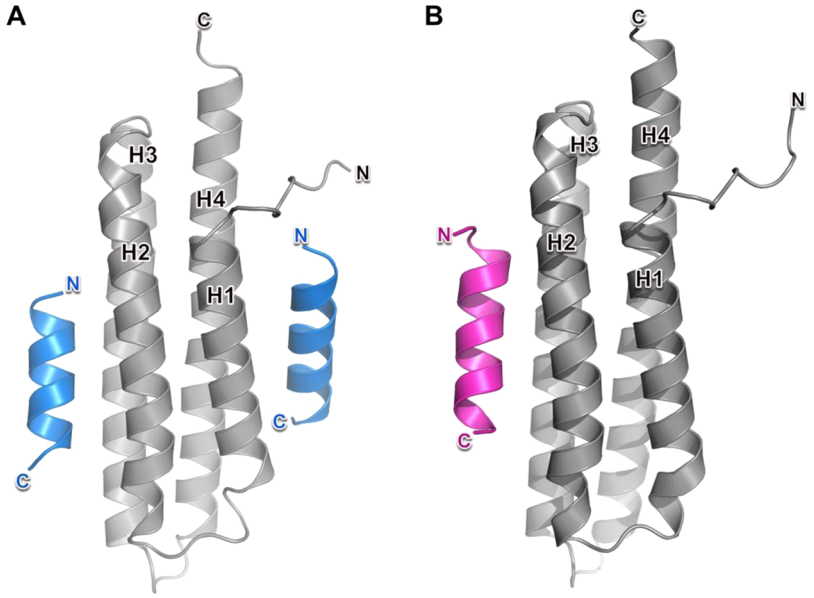

Figure 1. Crystal structures of Pyk2-FAT in complex with leupaxin's LD1 and LD4 motifs. Structures of the Pyk2-FAT/leupaxin-LD1 complex (A) and the Pyk2-FAT/leupaxin-LD4 complex (B) shown in cartoon representation. Pyk2-FAT is gray. Leupaxin-LD1 and leupaxin-LD4 peptides are blue and magenta, respectively. Secondary structure elements of Pyk2-FAT are labeled. Leupaxin-LD1 and leupaxin-LD4 peptides both form an amphipathic helix upon interaction with Pyk2-FAT. In the Pyk2-FAT/leupaxin-LD1 complex structure, two leupaxin-LD1 peptide molecules bind to Pyk2-FAT using the H1/H4 and H2/H3 sites. In the Pyk2-FAT/leupaxin-LD4 complex structure, one leupaxin-LD4 peptide molecule occupies the H2/H3 site of Pyk2-FAT.

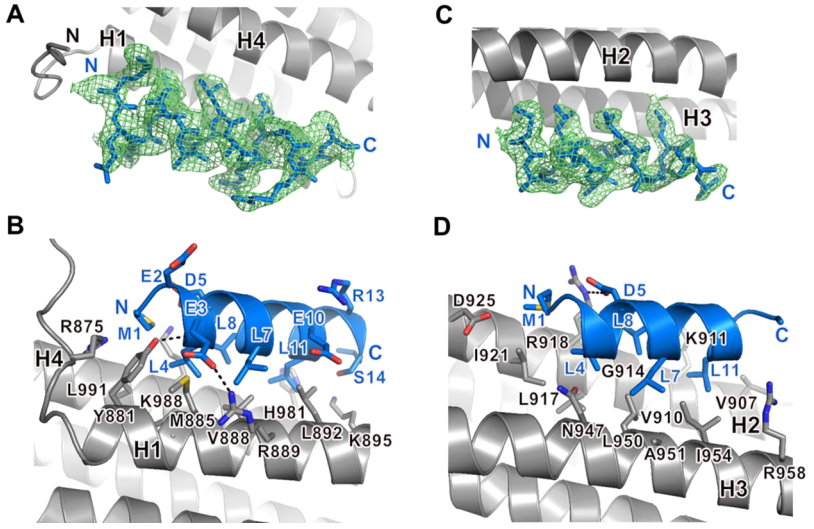

Figure 2. Structure of Pyk2-FAT bound to leupaxin's LD1 motif peptide. (A, C) $F_o - F_c$ simulated annealing omit density contoured at 2σ for leupaxin-LD1 peptide bound to H1/H4 and H2/H3 of Pyk2-FAT, respectively. Pyk2-FAT and leupaxin-LD1 peptide are gray and blue, respectively. Secondary structure elements of Pyk2-FAT are labeled. (B, D) Interaction of leupaxin-LD1 peptide with H1/H4 and H2/H3 of Pyk2-FAT, respectively. Peptide residues, along with important interacting residues from Pyk2-FAT, are shown as blue and gray sticks, respectively. Black dotted lines indicate hydrogen bonds.

Leupaxin LD Motifs Have Preferential Binding for Pyk2-FAT. We next decided to investigate the interaction between Pyk2 and leupaxin. Leupaxin has four LD motifs in its N-terminus, all of which can potentially interact with the Pyk2-FAT domain. On the basis of phylogenetic tree and sequence alignment analysis of leupaxin and paxillin using ClustalW,[56] we defined the nomenclature of leupaxin's LD motifs based on the LD motifs of paxillin (Figure S2) and thus named leupaxin's four LD motifs LD1, LD3, LD4, and LD5. As shown in Figure S2, although there is no leupaxin LD motif that is equivalent to the paxillin LD2 motif, the paxillin LD2 motif shares a stronger phylogenetic relationship with LD1 of leupaxin than with other LD motifs of leupaxin.

To examine the association between Pyk2 and leupaxin, we first generated four peptides corresponding to the four LD motifs of leupaxin, leupaxin-LD1 peptide (residues 1−20), leupaxin-LD3 peptide (residues 36−56), leupaxin-LD4 peptide (residues 86−104), and leupaxin-LD5 peptide (residues 125−150), and measured the binding affinity of the peptides to the Pyk2-FAT domain using ITC (Figure S3). We found that both leupaxin-LD1 and leupaxin-LD4 peptides bound to the Pyk2-FAT domain with a 2 to 1 stoichiometry; however, leupaxin-

DOI: 10.1021/acs.biochem.5b01274
Biochemistry 2016, 55, 1332−1345

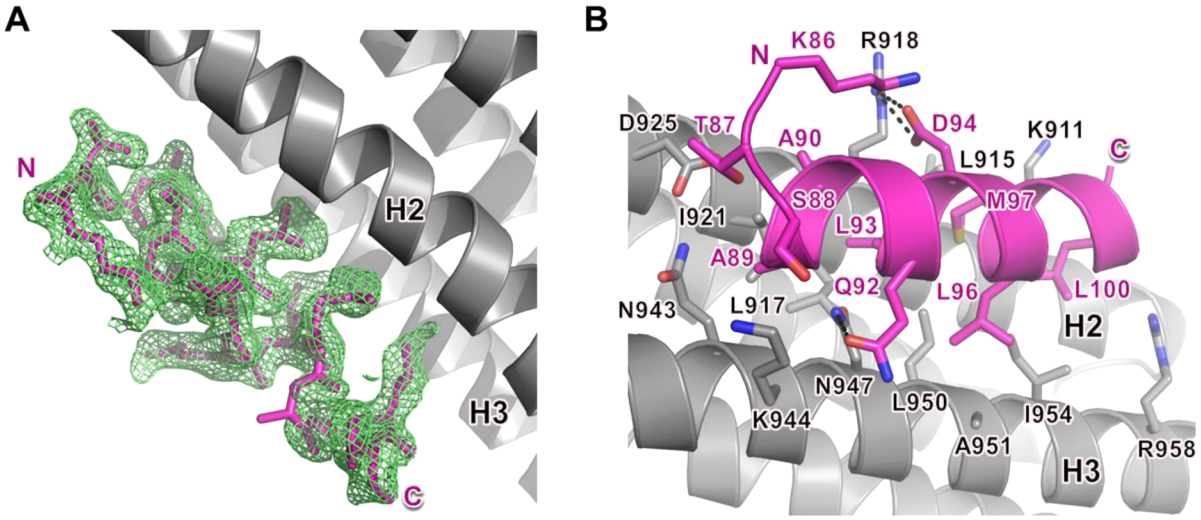

Figure 3. Structure of Pyk2-FAT bound to leupaxin-LD4 motif peptide. (A) $F_o - F_c$ simulated annealing omit density for Pyk2-FAT/leupaxin-LD4 contoured at 2σ. Pyk2-FAT and leupaxin-LD4 peptide are gray and light magenta, respectively. Secondary structure elements of Pyk2-FAT are labeled. (B) Interface between the Pyk2-FAT H2/H3 binding site and leupaxin-LD4 peptide. Leupaxin-LD4 peptide residues, along with important interacting residues from Pyk2-FAT, are shown as magenta and gray sticks, respectively. Black dotted lines indicate hydrogen bonds.

LD3 and leupaxin-LD5 peptides did not bind to the Pyk2-FAT domain. The binding data for both leupaxin-LD1 and leupaxin-LD4 could be fitted to a sequential two-site binding model (Table 1). For leupaxin-LD1, the binding affinity (K_D) was 2.8 μM to the first site and 52.0 μM to the second; similarly, for the leupaxin-LD4 peptide, the binding affinity was 2.2 μM to the first site and 33.0 μM to the second site.

Crystal Structural Study of Pyk2-FAT in Complex with Leupaxin-LD1 Peptide. To further investigate the molecular basis for leupaxin LD motif recognition by Pyk2-FAT, we cocrystallized Pyk2-FAT with the leupaxin-LD1 and leupaxin-LD4 peptides. A detailed analysis of Pyk2-FAT binding to leupaxin-LD1 and leupaxin-LD4 was performed, along with comparisons to previously reported Pyk2-FAT complexes with paxillin-LD2 and paxillin-LD4. The leupaxin-LD1 and leupaxin-LD4 complex structures were determined at 2.5 and 1.8 Å, respectively. Data collection and refinement statistics are shown in Table 2, and final simulated annealing omit density for the peptides is shown in Figures 2A,C and 3A. Both leupaxin-LD1 and leupaxin-LD4 peptides form amphipathic helices upon interaction with the four-helix bundle of Pyk2-FAT (Figure 1).

In the Pyk2-FAT/leupaxin-LD1 crystal structure, Pyk2-FAT binds two solvent-exposed leupaxin-LD1 peptides via its H1/H4 and H2/H3 surfaces. At the H1/H4 interface, we observed electron density for the first 15 residues of the 20-residue leupaxin-LD1 peptide (Met1−Thr15), with residues Glu2−Arg13 forming an amphipathic helix (Figure 2B). As predicted from previous FAK and Pyk2 structural studies with paxillin's LD motifs, hydrophobic interactions involving the leupaxin-LD1 core motif (^{4}LDXLLXXL^{11}) are important for complex stability. The side chains of conserved leucines 4, 7, 8, and 11 of leupaxin-LD1 make hydrophobic contacts with the side chains of Tyr881, Met885, Leu892, Ala984, Val888, Lys988, and Leu991 of Pyk2-FAT in a manner similar to what we and others have observed for structurally equivalent residues of paxillin-LD2 and paxillin-LD4 peptides in the previously reported Pyk2-FAT/paxillin-LD2 (pdb code: 4R32) and Pyk2-FAT/paxillin-LD4 complexes (PDB codes: 3GM1 and 3U3F). These leucines are invariant among the LD1, LD2, and LD4 motifs of paxillin and leupaxin, with the exception of Leu8 in leupaxin, which is equivalent to Met270 of paxillin LD4. The association of Pyk2-FAT and leupaxin-LD1 is further strengthened by interactions with amino acids immediately flanking the core leupaxin-LD1 motif sequence. Unique to leupaxin-LD1, N-terminal Met1 fills a shallow cavity on the H1/H4 surface created by Tyr881, Leu991, Lys988, Arg875, and Asp995. Also, the overall binding affinity and α-helical stability of the N-terminus of leupaxin-LD1 are likely strengthened by an intermolecular hydrogen bond between the amide moiety of Leu4 and the hydroxyl moiety of Tyr881 of Pyk2-FAT. In addition, Glu3 forms a hydrogen bond with Arg889. Although the side chain of the equivalent glutamate in paxillin-LD2 and paxillin-LD4 was not visible in our previously determined Pyk2-FAT/peptide structures (4R32 and 3U3F), modeling suggests that the interaction is structurally conserved. The Pyk2-FAT/paxillin-LD4 structure (3GM1) does not provide insight into this interaction because Glu265 of LD4 and Arg889 of Pyk2-FAT lie on opposite sides of an unrelated Pyk2-FAT molecule in the asymmetric unit. Finally, at the C-terminus of the bound leupaxin-LD1, Ser14 is observed in van der Waals contact with Lys911, with its side chain hydroxyl moiety forming an intermolecular hydrogen bond to the carbonyl oxygen of Leu11.

For comparison, a detailed structural analysis of leupaxin-LD1 binding at H2/H3 of Pyk2-FAT was also performed (Figure 2D). Electron density for the first 13 residues of the 20-residue leupaxin-LD1 peptide was observed (Met1−Arg13), wherein residues from Glu2 to Glu12 form an amphipathic helix on the H2/H3 surface (Figure 2C,D). Within the core of the leupaxin-LD1 motif, the same types of interactions were observed as those noted for H1/H4 binding. Specifically, side chains of conserved leucines 4, 7, and 11 form hydrophobic interactions with Leu917, Ile921, Leu950, Ala951, Ile954, and Val910 of Pyk2-FAT. Also, Leu8 is in van der Waals contact with Gly914 and Arg918. In addition, the highly conserved aspartate that defines the LD motif, Asp5, forms a hydrogen bond with Arg918. These core motif interactions are indeed conserved among Pyk2-FAT complex structures with paxillin-LD2 and paxillin-LD4 peptides. Compared to paxillin-LD2 and paxillin-LD4, however, leupaxin-LD1 interactions with Pyk2-

DOI: 10.1021/acs.biochem.5b01274
Biochemistry 2016, 55, 1332−1345

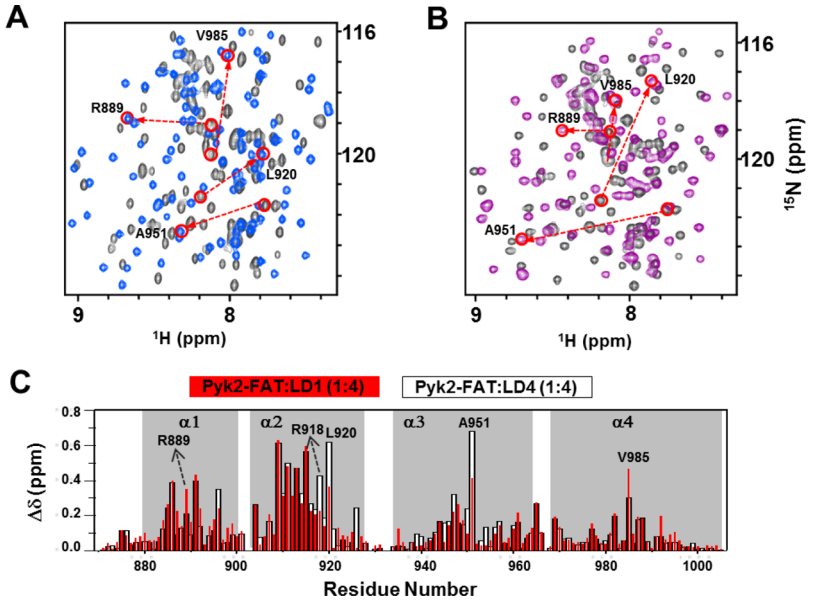

Figure 4. NMR analysis for binding of Pyk2-FAT to the high-affinity leupaxin-LD1 and leupaxin-LD4 peptides. (A, B) Superposition of $^{1}H-^{15}N$-HSQC spectra of Pyk2-FAT with leupaxin-LD1 and leupaxin-LD4 peptides added at different molar ratios is shown in black (1:0), blue (1:4 leupaxin-LD1), and magenta (1:4 leupaxin-LD4). (C) Histogram outlining the magnitude of the average chemical shift perturbation (CSP) of the ^{15}N and ^{1}H backbone amide resonances of Pyk2-FAT upon titration with leupaxin-LD1 and leupaxin-LD4 peptides. Red and black bars indicate chemical shift changes at 4 equiv of leupaxin-LD1 and leupaxin-LD4 peptides, respectively. Residues that show significant differences in the magnitude of CSP between additions of 4 equiv of leupaxin-LD1 and leupaxin-LD4 peptides are labeled. Helices 1−4 (H1−H4) are shown in gray.

FAT outside the core LD motif are sparse. Furthermore, leupaxin-LD1 makes limited interactions with H2/H3 compared to those with H1/H4. Only Met1 was observed to interact with the H2/H3 surface. Specifically, Met1 makes a hydrophobic contact with Ile921 and van der Waals interactions with Arg918, Gly922, and Asp925 from helix H2. Modeling suggests that Glu12 near the C-terminus of leupaxin-LD1 might also contribute to binding in solution; although the side chain of Glu12 was disordered and not included in the final structure, rotamer analysis places it in proximity to form a hydrogen bond with Lys911. Finally, comparison of leupaxin-LD1 binding at both Pyk2-FAT surfaces suggests that leupaxin-LD1 may bind tighter to the H1/H4 site than to the H2/H3 site.

Leupaxin-LD4 Binding at H2/H3. As a further probe of LD motif binding, detailed X-ray structural analysis of leupaxin-LD4 binding to Pyk2-FAT was performed. Despite adding a 4 M excess of leupaxin-LD4 peptide to the cocrystallization mixture, the stable complex that readily crystallized contained only one molecule of leupaxin-LD4 peptide bound to Pyk2-FAT. This result was somewhat unexpected as our ITC results indicate a 1:2 stoichiometry in solution with K_D's of 2.2 and 33.0 μM for the first and second peptide associations. The 1.8 Å Pyk2-FAT/leupaxin-LD4 structure contains leupaxin-LD4 bound at the H2/H3 site, wherein crystal packing blocked the H1/H4 site. This packing does not demonstrate an inability of leupaxin-LD4 to bind the H1/H4 site of Pyk2-FAT in solution, but it is highly suggestive that H2/H3 is a stronger affinity binding site. Furthermore, leupaxin-LD4 shares a strong sequence homology with paxillin-LD4. Therefore, there is no structural basis to suggest leupaxin-LD4 cannot bind the H1/H4 site in a manner similar to what was observed for Pyk2-FAT/paxillin-LD4 (3GM1 and 3U3F). Rather, it is likely that leupaxin-LD4, like paxillin-LD4, binds strongest to H2/H3. Electron density for the first 16 of 19 residues (Lys86−Thr101) from the solvent-exposed leupaxin-LD4 peptide was observed, with residues Ser88−Leu100 forming an amphipathic helix (Figure 3). The consensus core leupaxin-LD4 motif (^{93}LDXL-LXXL^{100}) displays the same structurally conserved interactions as those described earlier for leupaxin-LD1, paxillin-LD2, and paxillin-LD4. These involve hydrophobic contacts with conserved leucines 93, 96, and 100 and semiconserved Met97, as well as a hydrogen bond between the highly conserved Asp94 and Arg918 of Pyk2-FAT. Hydrophobic contacts are mediated by side chains from both α helices H2 and H3 of Pyk2-FAT; Val907, Val910, Lys911, Leu915, Leu917, and Ile921 from helix H2 and Leu950, Ala951, Ile954, and Met957 from helix H3 contribute to binding (Figure 3B).

Interactions between Pyk2-FAT H2/H3 and residues flanking the consensus core of leupaxin-LD4 motif further enhance complex formation (Figure 3B). Although N-terminal residue Lys86 is not involved in direct binding, it may enhance the helical stability of the leupaxin-LD4 peptide at the H2/H3 surface by mediating an intramolecular hydrogen bond to Asp94 while also packing against the helical turn formed by Ala90 and Ala91 of leupaxin-LD4. Interestingly, Lys86 is unique to leupaxin-LD4. Thr87 may also provide helical stability, and it contributes to peptide binding directly; the side chain hydroxyl moiety makes an intramolecular hydrogen bond to the amide moiety of Ala90, effectively serving as an N-terminal α-helical cap, while also forming a hydrogen bond to the side chain carboxylate of Asp925 from Pyk2-FAT. These dual roles for Thr87 may be present in paxillin-LD4 as it contains Ser260 at the equivalent position in the sequence alignment. Paxillin-LD2 does not have a Thr87 equivalent but, instead, contains a glycine residue. Ala89, common among LD4 of leupaxin and paxillin only, is in hydrophobic contact with Ile921 and is in van der Waals contact with Glu943, Lys944, and Asn947. Ala90 of LD4, which is structurally equivalent to

DOI: 10.1021/acs.biochem.5b01274
Biochemistry 2016, 55, 1332−1345

Met1 of LD1, is in hydrophobic contact with Ile921 and van der Waals contact with Asp925. In addition, semiconserved Gln92 forms a hydrogen bond with Asn947. This residue is a glutamate in leupaxin-LD1, paxillin-LD2, and paxillin-LD4.

Taken together, Pyk2-FAT/leupaxin-LD1 and Pyk2-FAT/leupaxin-LD4 complex structures provide detailed insight into how these two leupaxin LD motifs can interact in distinct ways despite the similarity of their core interaction regions. Differences in the core flanking sequences between leupaxin-LD1 and leupaxin-LD4 likely contribute to the selective association of these two leupaxin LD motifs for opposite binding surfaces on Pyk2-FAT. Most notably, leupaxin-LD1, starting with Met1, has three residues versus leupaxin-LD4 with seven residues prior to their common core. The extra helical turn for leupaxin-LD4 likely stabilizes the helix−helix interaction at H2/H3 and provides more opportunities to contact the H2/H3 surface relative to leupaxin-LD1. However, such a long helix would clash with Pyk2-FAT and has not been observed in paxillin-LD2 and paxillin-LD4 complexes, where Tyr881 and the N-terminus of Pyk2-FAT impose a steric restriction on continuation of the helix.[28,33−36] Therefore, the bound leupaxin-LD1 may represent the optimal helix, allowing a tighter helix−helix association with the H1/H4 site of Pyk2-FAT.

Mapping the Interaction between Pyk2-FAT and Leupaxin LD Motifs by NMR. Our combined X-ray crystal structure and ITC data analysis suggests that leupaxin-LD1 prefers the H1/H4 site over the H2/H3 site. Furthermore, leupaxin-LD4 likely binds to the H2/H3 site better than leupaxin-LD1 does. To further probe these differences between leupaxin-LD1 and leupaxin-LD4 in their association with Pyk2-FAT, we performed detailed binding studies using NMR. CSPs for either leupaxin-LD1 or leupaxin-LD4 bound to Pyk2-FAT were measured by adding unlabeled leupaxin-LD1 and leupaxin-LD4 peptides to ^{15}N-labeled Pyk2-FAT (Figure 4). Examining a series of ^{1}H−^{15}N correlation spectra of Pyk2-FAT in the presence of different concentrations of LD peptides (Pyk2/LD peptide ratios of 1:0.4, 1:0.8, 1:1.2, 1:1.6, 1:2.4, and 1:4), we observed that the binding sites for both leupaxin-LD1 and leupaxin-LD4 peptides are located to the central region of the solvent-exposed surfaces of H2/H3 and H1/H4. Pyk2-FAT solvent-exposed residues Glu904, Val909, Lys911, Val913, Leu915, Leu920, Lys944, Asn947, and Ala951 from H2/H3 and Glu886, Val888, Val891, Lys895, Thr982, and Val985 from H1/H4 exhibited significant perturbations after binding to leupaxin-LD1 and leupaxin-LD4 peptides (Figure 4).

Detailed chemical-shift perturbation analysis of leupaxin-LD1 and leupaxin-LD4 peptides bound to Pyk2-FAT was complicated by the ability of these two peptides to occupy both sites. Upon addition of 4 equiv of either leupaxin-LD1 or leupaxin-LD4 peptide, the HSQC spectrum underwent a drastic change that affected almost every peak in the spectrum (Figure 4A,B). Interestingly, an overlay of the Pyk2-FAT CSP plots for the addition of leupaxin-LD1 versus leupaxin-LD4 clearly shows that there are distinguishable disparities between the magnitude of CSP for critical residues at the H1/H4 and H2/H3 regions. These differences likely reflect the selectivity of these two motifs for opposite faces of Pyk2-FAT, as observed in the respective crystal structure complexes. For example, Arg889 and Val985 from the H1/H4 region of Pyk2-FAT show a high magnitude of CSP upon addition of leupaxin-LD1 compared to that with leupaxin-LD4 (Figure 4C). In the Pyk2-FAT/leupaxin-LD1 crystal structure, we observed that Arg889 forms a hydrogen bond with Glu3 of leupaxin-LD1 peptide, whereas Val985 is in close proximity to make hydrophobic contact with Leu8 and Leu11 of leupaxin-LD1 peptide. Similarly, residues Arg918 and Ala951 from H2/H3 show a high magnitude of CSP upon addition of leupaxin-LD4 relative to leupaxin-LD1 (Figure 4C). The crystal structure of Pyk2-FAT/leupaxin-LD4 indeed supports that Arg918 forms hydrogen bond with conserved Asp94 of leupaxin-LD4 peptide and that Ala951 makes hydrophobic interaction with Leu96 of leupaxin-LD4 peptide. Interestingly, previous analogous studies with paxillin show no differences in the relative Pyk2-FAT CSP upon adding paxillin-LD2 or paxillin-LD4. Furthermore, we observed that both paxillin LD2 and LD4 motifs compete equally for H2/H3.[36] The CSP differences observed for leupaxin's LD motifs may result from direct interaction of leupaxin-LD1 and leupaxin-LD4 peptides at H1/H4 and H2/H3 sites, respectively. Therefore, our NMR studies suggest that Pyk2-FAT/leupaxin likely forms a stable complex.

Full-Length Leupaxin Binding to Pyk2-FAT. The results of the peptide-binding experiments demonstrate that leupaxin-LD1 and leupaxin-LD4 can dock to two distinct sites on the Pyk2-FAT domain. In order to explore full-length leupaxin interaction with Pyk2-FAT, we expressed a leupaxin construct comprising LD1−LD5 motifs (leupaxin$^{1-151}$). We then determined the stoichiometry of the Pyk2-FAT/leupaxin$^{1-151}$ complex in solution using SEC-MALS. The complex resolved as a single peak with a molecular mass of 29.5 kDa, indicating the existence of a 1:1 complex of Pyk2-FAT to leupaxin$^{1-151}$ (theoretical mass of 33.6 kDa) (Figure S4).

We then used ITC to study the association of Pyk2-FAT with a truncated leupaxin construct comprising LD1−LD4 motifs (leupaxin$^{1-105}$) since leupaxin-LD5 peptide had no detectable binding for Pyk2-FAT (Table 1). Representative plots for each titration are shown in Figure S5, and a summary of the thermodynamic parameters is given in Table 1. The data best fit to a single-site model assuming 1:1 stoichiometry with a K_D of approximately 0.6 μM. This apparent 1:1 complex formation is consistent with the stoichiometry observed for the Pyk2-FAT/leupaxin$^{1-151}$ complex by SEC-MALS. Interestingly, the binding affinity of Pyk2-FAT for leupaxin$^{1-105}$ is approximately 4−5-fold higher than that for leupaxin-LD1 and leupaxin-LD4 peptides alone.

To further probe this interaction, we performed an NMR CSP experiment. During NMR titration of unlabeled leupaxin$^{1-105}$ to ^{15}N-labeled Pyk2-FAT (Pyk2-FAT/leupaxin$^{1-105}$ ratios of 1:0.4, 1:0.8, 1:1.2, and 1:2.4), most of the amide resonances from the H1/H4 and H2/H3 sites disappeared below the limit of detection. This peak disappearance is due to an intermediate slow exchange regime, indicating tight peptide binding at the H1/H4 and H2/H3 sites. Upon addition of excess leupaxin$^{1-105}$ to Pyk2-FAT (1:2), most of the resonances reappeared in the spectrum, suggesting the formation of a stable complex between Pyk2-FAT and leupaxin$^{1-105}$ (Figure S6). However, we observed limited NOEs, hindering structure determination. Although the backbone resonances of this complex could be assigned, the lack of strong NOEs may be due to the slower tumbling of the large Pyk2-FAT/leupaxin$^{1-105}$ complex. To examine whether leupaxin$^{1-105}$ binding to Pyk2-FAT forms a stable complex, ^{1}H−^{15}N-TROSY spectra of Pyk2-FAT bound to leupaxin$^{1-105}$ and Pyk2-FAT bound to a leupaxin-LD1 and leupaxin-LD4 mixture (1:1) were overlaid (Figure S7). The spectra overlay extremely well, suggesting that Pyk2-FAT binding to

DOI: 10.1021/acs.biochem.5b01274
Biochemistry 2016, 55, 1332−1345

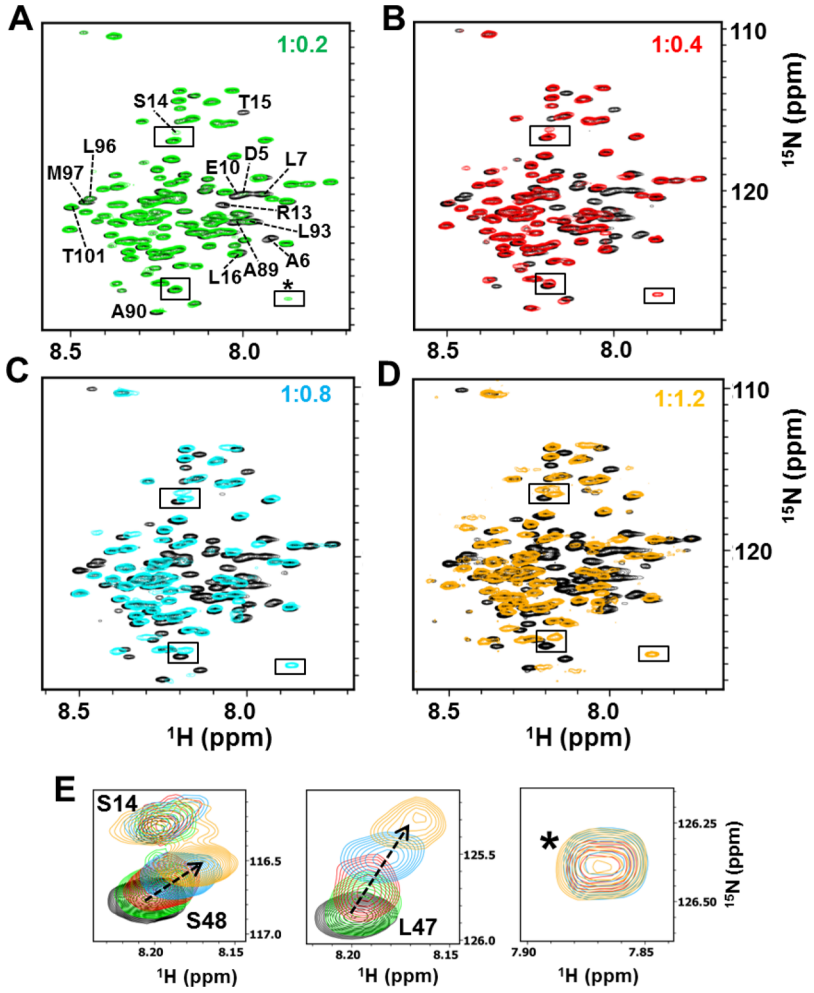

Figure 5. Mapping the leupaxin$^{1-105}$ and Pyk2-FAT interaction using NMR spectroscopy. (A–D) Superposition of ^{1}H–^{15}N-TROSY-HSQC spectra of leupaxin$^{1-105}$ (residues 1–105) with unlabeled Pyk2-FAT added at different molar ratios is shown in black (1:0), green (1:0.4), red (1:0.8), cyan (1:1.6), and yellow (1:2.4). Upon titration of Pyk2-FAT to labeled leupaxin$^{1-105}$, most residues from leupaxin-LD1 and leupaxin-LD4 motifs (labeled with dashed lines in panel A) disappeared below the limit of detection due to slow exchange. This phenomenon is indicative of tight binding between high-affinity LD motifs and Pyk2-FAT. The boxed peaks are described in panel E. (E) Overlay of spectra from selected residues corresponding to boxed peaks in panels A–D. L47 and S48, which reside in the loop between leupaxin-LD1 and leupaxin-LD3 motifs, exhibit fast exchange. This phenomenon may be attributed to indirect effects arising from structural rearrangements of loops upon leupaxin-LD1 and leupaxin-LD4 motifs binding with Pyk2-FAT. S14 from leupaxin-LD1 motif and the unassigned new peak labeled with an asterisk represent residues in slow exchange.

leupaxin$^{1-105}$ closely resembles Pyk2-FAT binding to a 1:1 mixture of leupaxin-LD1 and leupaxin-LD4 peptides (Pyk2-FAT/leupaxin-LD1 + leupaxin-LD4) in solution. This experiment also confirms that leupaxin$^{1-105}$ loops and LD3 motif residues are not involved in binding.

We also performed reverse NMR titration by adding unlabeled Pyk2-FAT to ^{15}N-labeled leupaxin$^{1-105}$. During titration, most of the amide resonances from the LD1 and LD4 motifs disappeared below the limit of detection due to a slow exchange interaction with Pyk2-FAT, which is indicative of tight binding. At a 1:2.4 ratio of leupaxin$^{1-105}$ to Pyk2-FAT, some of the peaks reappear in the spectra. However, they are weak in intensity, presumably due to the slow tumbling of the large complex, which precluded backbone assignment and structure determination of the complex (Figure 5). The large loop regions that connect the LD motifs may contribute to increasing the effective overall volume of the complex, further reducing the expected tumbling relative to a globular complex of the same molecular mass. Interestingly, during titration, we observed that residues residing in the loops between LD motifs exhibit chemical shift perturbation (Figure 5E). These loop residue peak shifts may be attributed to indirect effects arising from structural rearrangements of loops upon binding of the LD1 and LD4 motifs of leupaxin to Pyk2-FAT.

Leupaxin-LD1 and Leupaxin-LD4 Binding to Pyk2-FAT. To further assess the structure of the Pyk2-FAT domain in complex with both LD1 and LD4 motifs simultaneously, we designed a fusion construct by linking the leupaxin-LD1 motif at the C-terminus of Pyk2-FAT. Critical to the design, the optimized linker should not interfere with the interaction between the attached LD1 motif and the H1/H4 site of Pyk2-FAT. For this purpose, we generated three fusion constructs with various linker lengths. Among these constructs, the fusion protein containing an 8-residue linker (GGSGGGGG) exhibited the best quality ^{1}H–^{15}N-HSQC spectrum compared to that with a 6-residue (GGSGGG) or 11-residue (GGSGGGGGGSG) linker (Figure S8), indicating that the LD1 motif of leupaxin within this fusion protein bound to the H1/H4 binding site of the Pyk2-FAT solidly. We term this fusion protein Pyk2-FAT-LD1.

DOI: 10.1021/acs.biochem.5b01274
Biochemistry 2016, 55, 1332–1345

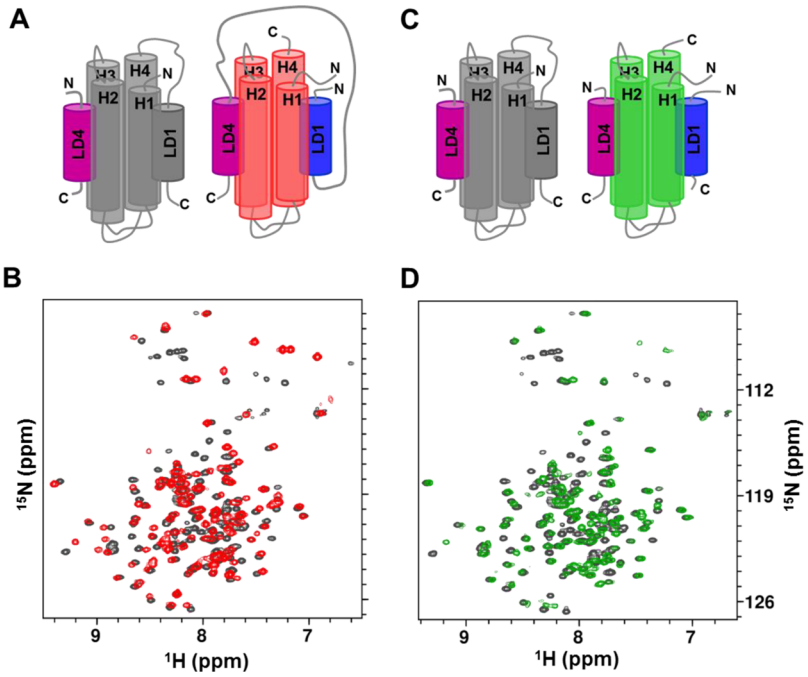

Figure 6. NMR spectra of Pyk2-FAT bound to a full-length leupaxin mimic. (A) Cartoon representation depicting Pyk2-FAT-LD1/leupaxin-LD4 (Pyk2-FAT-LD1 in dark gray) and Pyk2-FAT/leupaxin$^{1-105}$ (Pyk2-FAT in red). (B) ^{1}H−^{15}N-TROSY spectrum of Pyk2-FAT-LD1/leupaxin-LD4 at (1:2) (dark gray) with the ^{1}H−^{15}N-TROSY spectrum of Pyk2-FAT/leupaxin$^{1-105}$ (red) superimposed. (C) Cartoon representation depicting Pyk2-FAT-LD1/leupaxin-LD4 (Pyk2-FAT-LD1 in dark gray) and Pyk2-FAT/leupaxin-LD1 + leupaxin-LD4 (Pyk2-FAT in green). (D) ^{1}H−^{15}N-TROSY spectrum of Pyk2-FAT-LD1/leupaxin-LD4 (1:2 ratio) (dark gray) with the ^{1}H−^{15}N-TROSY spectrum of Pyk2-FAT/leupaxin-LD1 + leupaxin-LD4 (1:2.4 ratio) (green) superimposed.

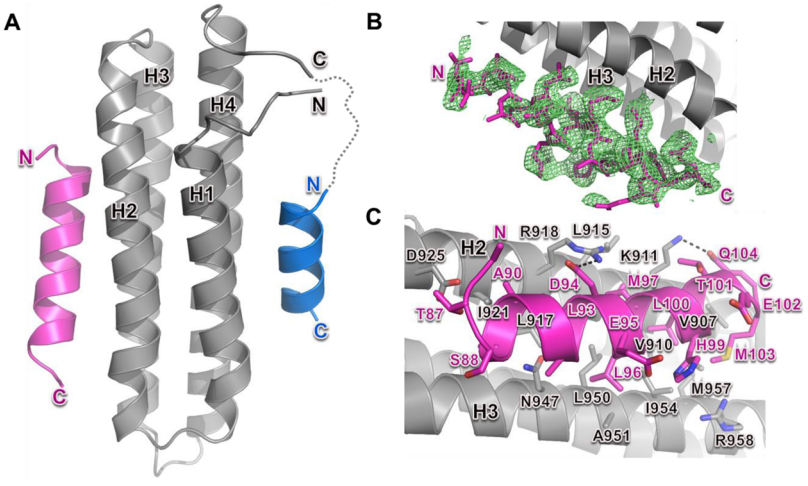

Figure 7. Complex structure of Pyk2-FAT-LD1 bound to leupaxin's LD4 motif. (A) Crystal structure of Pyk2-FAT-LD1 bound to leupaxin-LD4 peptide. Pyk2-FAT is gray. Leupaxin-LD1 and leupaxin-LD4 peptides are blue and magenta, respectively. Secondary structure elements of Pyk2-FAT are labeled. The dotted line indicates the unobserved glycine-rich linker between the C-terminus of Pyk2-FAT and the leupaxin-LD1 motif. (B) $F_o - F_c$ simulated annealing omit density, contoured at 2σ, for leupaxin-LD4 peptide bound at H2/H3 of Pyk2-FAT. (C) Interface between the H2/H3 binding site of Pyk2-FAT and leupaxin-LD4 peptide. Leupaxin-LD4 peptide residues, along with important interacting residues from Pyk2-FAT, are shown as magenta and gray sticks, respectively. Black dotted lines indicate hydrogen bonds.

With the Pyk2-FAT-LD1 construct in hand, we first asked whether there is any preferential association between leupaxin's LD1 and LD4 motifs to the open H2/H3 site of the Pyk2-FAT in the fusion construct. To address this question, we first measured binding affinities of both leupaxin-LD1 and leupaxin-LD4 peptides to Pyk2-FAT-LD1 respectively by ITC. Representative titrations are shown in Figure S9, and the thermodynamic parameters of binding are listed in Table S1. As expected, the experimental data for leupaxin-LD4 peptide binding to Pyk2-FAT-LD1 best fit to a one-site binding model, with an estimated $K_D \sim 2\ \mu$M. However, leupaxin-LD1 peptide binding to Pyk2-FAT-LD1 appears to be very weak compared to leupaxin-LD4 peptide, and thus a reliable K_D measurement could not be obtained.

We also used CSP to study the interaction between leupaxin-LD1 and leupaxin-LD4 peptides with Pyk2-FAT-LD1. NH backbone resonances of Pyk2-FAT-LD1 were assigned based on the three-dimensional HNCO, HNCA, CBCA(CO)NH,

DOI: 10.1021/acs.biochem.5b01274
Biochemistry 2016, 55, 1332−1345

and HNCACB spectra. We then collected $^{1}H-^{15}N$-HSQC during the titration of leupaxin-LD1 and leupaxin-LD4 peptides to ^{15}N-labeled Pyk2-FAT-LD1 (Pyk2-FAT-LD1/LD1 or LD4 ratios of 1:0, 1:0.4, 1:0.8, 1:1.2, 1:1.6, and 1:2). During NMR titration of LD4 to Pyk2-FAT-LD1, most of the amide resonances from the H2/H3 site undergo intermediate slow exchange, indicating tight peptide binding at the H2/H3 region (Figure S10A). However, during the titration of leupaxin-LD1 peptide to Pyk2-FAT-LD1, most of the amide resonances from the H2/H3 binding site undergo fast exchange, indicating weak peptide binding at the H2/H3 region (Figure S10B).

Although both ITC and CSP data for leupaxin-LD1 and leupaxin-LD4 peptide binding to Pyk2-FAT-LD1 supported the notion that H2/H3 is the preferential binding site for leupaxin-LD4 in the context of the native Pyk2-FAT/leupaxin complex, an overlay of the $^{1}H-^{15}N$-TROSY spectra for the Pyk2-FAT-LD1/leupaxin-LD4 complex and Pyk2-FAT/leupaxin$^{1-105}$ shows that they are indeed very similar (Figure 6A,B). Furthermore, an overlay of the $^{1}H-^{15}N$-TROSY spectra for the Pyk2-FAT-LD1/leupaxin-LD4 complex and the spectrum of Pyk2-FAT bound to a 1:1 mixture of leupaxin-LD1 and leupaxin-LD4 peptides (Pyk2-FAT/leupaxin-LD1 + leupaxin-LD4) is also very similar (Figure 6C,D). We therefore conclude that the leupaxin-LD4 peptide likely binds to Pyk2-FAT-LD1 in the same way as the LD4 motif of full-length leupaxin.

We next exploited the Pyk2-FAT-LD1 fusion construct for cocrystallization with leupaxin-LD4 peptide because this complex is a close approximate of the full-length leupaxin/Pyk2-FAT complex. The cocrystal structure of Pyk2-FAT-LD1 bound to leupaxin-LD4 peptide was determined at 2.0 Å resolution (Figure 7A). Data collection and refinement statistics are shown in Table 2, and final simulated annealing omit density for peptides is shown in Figure 7B for LD4 and Figure S11A for LD1. Two copies of the protein/peptide complex were observed in the asymmetric unit, corresponding to a 1:1 association of Pyk2-FAT to leupaxin-LD4. As expected, the fusion LD1 motif of leupaxin binds at the H1/H4 surface, whereas LD4 binds at the H2/H3 site. At the H1/H4 interface, electron density was observed for residues Met1−Arg13 of the C-terminal-linked leupaxin LD1 motif. Most of the interactions between Pyk2-FAT and linked LD1 residues were similar to those observed for Pyk2-FAT bound to leupaxin-LD1 peptide (Figure S11B). Interestingly, at the H2/H3 interface of Pyk2-FAT-LD1, we observed electron density for the entire leupaxin-LD4 peptide (Figure 7B). This included three additional residues not observed in the Pyk2-FAT/leupaxin-LD4 structure (Figures 7C and S11C). Likely stabilized by crystal packing, these residues form an extra helical turn at the C-terminus. In addition to extending the helix−helix interface, these residues make key interactions with the H2/H3 site of Pyk2-FAT-LD1. Met103 makes hydrophobic contact with Met957 and van der Waals interactions with Arg958 and Gln961. Also, Gln104 of leupaxin-LD4 makes van der Waals contact with Val907 and a hydrogen bond with Lys911 of Pyk2-FAT (Figure 7C).

DISCUSSION

Pyk2 overexpression has been associated with tumor progression in several cancers.[6,8,57,58] Furthermore, studies have shown that Pyk2 and leupaxin, a member of the paxillin family of proteins, form a functional complex in human cancers.[37,38] Like paxillin, leupaxin also contains LD motifs in its N-terminal region, and using biochemical, biophysical, and crystallographic techniques, we have demonstrated that two of the four leupaxin LD motifs directly bind to Pyk2. Previous reports showed that the Pyk2-FAT domain utilizes its H1/H4 and H2/H3 sites for the interaction with paxillin's LD2 and LD4 motifs.[34,36] However, there is no selectivity difference among the peptides; both bind with a 5-fold preference for the H2/H3 site (K_D: paxillin-LD2 = 6.9 μM; paxillin-LD4 = 8.0 μM) relative to the H1/H4 site (K_D: paxillin-LD2 = 35.2 μM; paxillin-LD4 = 46.3 μM). Furthermore, LD2 and LD4 exhibit roughly the same affinity for H2/H3, and this nonselective behavior likely contributes to the dynamic nature of the full-length paxillin/Pyk2-FAT complex.[36] However, using NMR titrations, here we found that leupaxin's LD1 and LD4 motifs exhibited a strong preference for the H1/H4 and H2/H3 sites of Pyk2-FAT, respectively (Figure 4). We propose that this is likely due to differences in specific residues that mainly reside outside of their common core LD motifs. Indeed, our structural analysis reveals that residues N-terminal to the core leupaxin LD4 motif (^{86}KTSA^{89}) enhance the affinity for the H2/H3 site relative to the LD1 motif of leupaxin that is devoid of these key residues at its N-terminus. In contrast, we reason that these additional residues at the N-terminus of the LD4 motif may sterically hinder binding at H1/H4 and render weak association relative to leupaxin-LD1 (Figure S12). Furthermore, in the context of full-length leupaxin, we propose that such a steric occlusion would likely be even more pronounced and that leupaxin-LD1 may represent the optimal helical length for Pyk2-FAT binding at the H1/H4 site of Pyk2.

To further examine the interaction between leupaxin and Pyk2, we expressed leupaxin$^{1-105}$ (comprising the LD1-LD3-LD4 region) and performed binding studies with Pyk2-FAT. Our ITC results show that there is a 4−5-fold increase in the binding affinity of leupaxin$^{1-105}$ for Pyk2-FAT relative to that of free leupaxin LD motifs (Table 1). This binding affinity of leupaxin$^{1-105}$ for Pyk2-FAT is 3-fold higher than that of paxillin$^{133-290}$ (which comprises LD2-LD3-LD4 motifs) to Pyk2-FAT.[36] In addition, our comprehensive structural and biophysical studies confirm that Pyk2-FAT and leupaxin$^{1-105}$ form a stable 1:1 complex in solution. Indeed, our extensive NMR studies support the hypothesis that leupaxin binds Pyk2-FAT in a concerted fashion. This discrete binding mechanism is in striking contrast to what we previously observed for Pyk2-FAT and paxillin$^{133-290}$, where complex formation, mediated by paxillin's LD2 and LD4 motifs, is highly dynamic and composed of two equally competing conformations.[36] On the other hand, in this study, we show that leupaxin-LD1 binds to H1/H4 of Pyk2-FAT about 13-fold stronger than paxillin-LD2 does and 17-fold stronger than paxillin-LD4 does. Likewise, leupaxin-LD4 binds H2/H3 about 3−4-fold stronger than paxillin-LD2 or paxillin-LD4 does. Furthermore, both leupaxin-LD1 and leupaxin-LD4 are able to discriminate the two LD-binding sites of Pyk2-FAT, exhibiting about 15- and 19-fold higher affinities, respectively, at their preferred Pyk2-FAT binding site. The binding specificities of both LD motifs of leupaxin likely contribute to the stable interaction between leupaxin and Pyk2.

Pyk2 is a homologue of FAK; it can functionally replace FAK in certain biological processes where FAK is limited.[17,19] However, the two proteins are not exactly the same. Structural studies of the FAT domains of the proteins in complex with paxillin showed that there are clear differences between the two proteins: Paxillin forms a stable complex with the FAK-FAT domain, whereas the interaction between paxillin and the Pyk2-FAT domain is very dynamic, likely due to the nearly equal

DOI: 10.1021/acs.biochem.5b01274
Biochemistry 2016, 55, 1332−1345

binding affinities of paxillin-LD2 and paxillin-LD4 to the H2/H3 site of Pyk2-FAT.[33,36] This competition does not exist in the FAK-FAT/paxillin complex; paxillin-LD2 has a severely reduced ability to bind H2/H3 of FAK-FAT due to the sequence differences between FAK-FAT and Pyk2-FAT, especially the residues comprising H3 within the H2/H3 binding site.[33,36] Like FAK and Pyk2, leupaxin is a functionally distinct homologue of paxillin. Leupaxin was identified as the binding partner of Pyk2.[37] Indeed, in many cells, including the breast cancer cells examined in this study, gene expression of Pyk2 and leupaxin is closely correlated. Like paxillin, leupaxin uses its N-terminal LD motifs to interact with Pyk2. However, unlike paxillin, in this study, we found that the leupaxin complex formed with Pyk2 is very stable; the interaction between leupaxin and Pyk2 strikingly resembles the interaction between paxillin and FAK.[33] Therefore, our study not only further confirms from a structural biology point of view that leupaxin is the native binding partner of Pyk2, whereas the biological binding partner of paxillin is FAK, but also sheds light on the complexity and specificity of supramolecular focal adhesion assemblies involving diverse protein−protein recognition events.

■ ASSOCIATED CONTENT

Supporting Information

The Supporting Information is available free of charge on the ACS Publications website at DOI: 10.1021/acs.biochem.5b01274.

Pearson correlation analysis in primary breast tumors; phylogenetic tree and multiple-sequence alignment analysis for the conserved LD motifs in leupaxin and paxillin; ITC of Pyk2-FAT binding to leupaxin LD1, LD3, LD4, and LD5 peptides; SEC-MALS data; leupaxin$^{1-105}$ binding to Pyk2-FAT data; comparison of $^{1}H-^{15}N$-HSQC spectra of Pyk2-FAT/leupaxin$^{1-105}$ with Pyk2-FAT/leupaxin-LD1 + leupaxin-LD4 and of Pyk2-FAT-LD1 construct with different linker lengths; ITC and NMR of Pyk2-FAT-LD1 binding to leupaxin LD1 and LD4 peptides; structural comparison of Pyk2-FAT/LD1 and Pyk2-FAT/LD4 with Pyk2-FATLD1 and Pyk2-FAT-LD1/LD4; preferential association of leupaxin LD1 and LD4 motifs on the Pyk2-FAT surface; expression and purification of the leupaxin$^{1-105}$; thermodynamic parameters for binding of Pyk2-FAT-LD1 to leupaxin LD1 and LD4 peptides obtained by ITC (PDF)

Accession Codes

Atomic coordinates and structure factors have been deposited in the Protein Data Bank with accession code 4XEF for the Pyk2-FAT/Leupaxin-LD1 complex, 4XEK for the Pyk2-FAT/Leupaxin-LD4 complex, and 4XEV for the Pyk2-FAT-LD1/Leupaxin-LD4 complex.

■ AUTHOR INFORMATION

Corresponding Authors

*(D.J.M.) E-mail: darcie.miller@stjude.org. Telephone: (901) 595-6277.

*(J.J.Z.) E-mail: jzheng@jsei.ucla.edu. Telephone: (310) 206-2173.

Funding

This work was supported by NIH grants GM100909 and CA21765 (Cancer Center Support Grant) and by Research to Prevent Blindness. Use of the Advanced Photon Source was supported by the U.S. Department of Energy, Office of Science, Office of Basic Energy Sciences, under Contract No. W-31-109-Eng-38.

Notes

The authors declare no competing financial interest.

■ ACKNOWLEDGMENTS

We thank Drs. Christy R. R. Grace and Weixing Zhang for NMR assistance and Drs. Patrick Rodrigues and Robert Cassell for peptide synthesis. X-ray diffraction data were collected at Southeast Regional Collaborative Access Team (SER-CAT) beamlines 22-ID and 22-BM at the Advanced Photon Source, Argonne National Laboratory. Supporting institutions may be found at www.ser-cat.org/members.html.

■ ABBREVIATIONS

Pyk2, proline-rich tyrosine kinase 2; FAK, focal adhesion kinase; FA, focal adhesion; GEO, Gene Expression Omnibus; ITC, isothermal titration calorimetry; HSQC, heteronuclear single quantum coherence; NOE, nuclear Overhauser enhancement; TROSY, transverse relaxation optimized spectroscopy; FAT, focal adhesion targeting; SE, sedimentation equilibrium; CSP, chemical shift perturbation; CARA, computer aided resonance assignment; MES, 4-morpholineethanesulfonic acid; SER-CAT, Southeast Regional Collaborative Access Team

■ REFERENCES

(1) Avraham, S., London, R., Fu, Y., Ota, S., Hiregowdara, D., Li, J., Jiang, S., Pasztor, L. M., White, R. A., and Groopman, J. E. (1995) Identification and characterization of a novel related adhesion focal tyrosine kinase (RAFTK) from megakaryocytes and brain. *J. Biol. Chem. 270*, 27742−27751.

(2) Herzog, H., Nicholl, J., Hort, Y. J., Sutherland, G. R., and Shine, J. (1996) Molecular cloning and assignment of FAK2, a novel human focal adhesion kinase, to 8p11.2-p22 by nonisotopic in situ hybridization. *Genomics 32*, 484−486.

(3) Lev, S., Moreno, H., Martinez, R., Canoll, P., Peles, E., Musacchio, J. M., Plowman, G. D., Rudy, B., and Schlessinger, J. (1995) Protein tyrosine kinase PYK2 involved in Ca(2+)-induced regulation of ion channel and MAP kinase functions. *Nature 376*, 737−745.

(4) Sasaki, H., Nagura, K., Ishino, M., Tobioka, H., Kotani, K., and Sasaki, T. (1995) Cloning and characterization of cell adhesion kinase beta, a novel protein-tyrosine kinase of the focal adhesion kinase subfamily. *J. Biol. Chem. 270*, 21206−21219.

(5) Le, H. T., Maksumova, L., Wang, J., and Pallen, C. J. (2006) Reduced NMDA receptor tyrosine phosphorylation in PTPalpha-deficient mouse synaptosomes is accompanied by inhibition of four src family kinases and Pyk2: an upstream role for PTPalpha in NMDA receptor regulation. *J. Neurochem. 98*, 1798−1809.

(6) Paulino, V. M., Yang, Z., Kloss, J., Ennis, M. J., Armstrong, B. A., Loftus, J. C., and Tran, N. L. (2010) TROY (TNFRSF19) is overexpressed in advanced glial tumors and promotes glioblastoma cell invasion via Pyk2-Rac1 signaling. *Mol. Cancer Res. 8*, 1558−1567.

(7) Sun, C. K., Ng, K. T., Sun, B. S., Ho, J. W., Lee, T. K., Ng, I., Poon, R. T., Lo, C. M., Liu, C. L., Man, K., and Fan, S. T. (2007) The significance of proline-rich tyrosine kinase2 (Pyk2) on hepatocellular carcinoma progression and recurrence. *Br. J. Cancer 97*, 50−57.

(8) Zhang, Y., Moschetta, M., Huynh, D., Tai, Y. T., Zhang, Y., Zhang, W., Mishima, Y., Ring, J. E., Tam, W. F., Xu, Q., Maiso, P., Reagan, M., Sahin, I., Sacco, A., Manier, S., Aljawai, Y., Glavey, S., Munshi, N. C., Anderson, K. C., Pachter, J., Roccaro, A. M., and Ghobrial, I. M. (2014) Pyk2 promotes tumor progression in multiple myeloma. *Blood 124*, 2675−2686.

(9) Parsons, J. T. (2003) Focal adhesion kinase: the first ten years. *J. Cell Sci. 116*, 1409−1416.

DOI: 10.1021/acs.biochem.5b01274
Biochemistry 2016, 55, 1332−1345

(10) Avraham, H., Avraham, S., and Taniguchi, Y. (2000) Receptor protein tyrosine phosphatases in hematopoietic cells. *J. Hematother. Stem Cell Res. 9*, 425−432.
(11) Schaller, M. D., and Sasaki, T. (1997) Differential signaling by the focal adhesion kinase and cell adhesion kinase beta. *J. Biol. Chem. 272*, 25319−25325.
(12) Klingbeil, C. K., Hauck, C. R., Hsia, D. A., Jones, K. C., Reider, S. R., and Schlaepfer, D. D. (2001) Targeting Pyk2 to beta 1-integrin-containing focal contacts rescues fibronectin-stimulated signaling and haptotactic motility defects of focal adhesion kinase-null cells. *J. Cell Biol. 152*, 97−110.
(13) Tokiwa, G., Dikic, I., Lev, S., and Schlessinger, J. (1996) Activation of Pyk2 by stress signals and coupling with JNK signaling pathway. *Science 273*, 792−794.
(14) Mitra, S. K., Hanson, D. A., and Schlaepfer, D. D. (2005) Focal adhesion kinase: in command and control of cell motility. *Nat. Rev. Mol. Cell Biol. 6*, 56−68.
(15) Yin, B. (2011) Focal adhesion kinase as a target in the treatment of hematological malignancies. *Leuk. Res. 35*, 1416−1418.
(16) Zhao, J., Zheng, C., and Guan, J. (2000) Pyk2 and FAK differentially regulate progression of the cell cycle. *J. Cell Sci. 113*, 3063−3072.
(17) Fan, H., and Guan, J. L. (2011) Compensatory function of Pyk2 protein in the promotion of focal adhesion kinase (FAK)-null mammary cancer stem cell tumorigenicity and metastatic activity. *J. Biol. Chem. 286*, 18573−18582.
(18) Sieg, D. J., Ilic, D., Jones, K. C., Damsky, C. H., Hunter, T., and Schlaepfer, D. D. (1998) Pyk2 and Src-family protein-tyrosine kinases compensate for the loss of FAK in fibronectin-stimulated signaling events but Pyk2 does not fully function to enhance FAK- cell migration. *EMBO J. 17*, 5933−5947.
(19) Weis, S. M., Lim, S. T., Lutu-Fuga, K. M., Barnes, L. A., Chen, X. L., Gothert, J. R., Shen, T. L., Guan, J. L., Schlaepfer, D. D., and Cheresh, D. A. (2008) Compensatory role for Pyk2 during angiogenesis in adult mice lacking endothelial cell FAK. *J. Cell Biol. 181*, 43−50.
(20) Guinamard, R., Okigaki, M., Schlessinger, J., and Ravetch, J. V. (2000) Absence of marginal zone B cells in Pyk-2-deficient mice defines their role in the humoral response. *Nat. Immunol. 1*, 31−36.
(21) Brown, M. C., Perrotta, J. A., and Turner, C. E. (1996) Identification of LIM3 as the principal determinant of paxillin focal adhesion localization and characterization of a novel motif on paxillin directing vinculin and focal adhesion kinase binding. *J. Cell Biol. 135*, 1109−1123.
(22) Brown, M. C., and Turner, C. E. (2004) Paxillin: adapting to change. *Physiol. Rev. 84*, 1315−1339.
(23) Thomas, J. W., Cooley, M. A., Broome, J. M., Salgia, R., Griffin, J. D., Lombardo, C. R., and Schaller, M. D. (1999) The role of focal adhesion kinase binding in the regulation of tyrosine phosphorylation of paxillin. *J. Biol. Chem. 274*, 36684−36692.
(24) Schlaepfer, D. D., Mitra, S. K., and Ilic, D. (2004) Control of motile and invasive cell phenotypes by focal adhesion kinase. *Biochim. Biophys. Acta, Mol. Cell Res. 1692*, 77−102.
(25) Tachibana, K., Sato, T., D'Avirro, N., and Morimoto, C. (1995) Direct association of pp125FAK with paxillin, the focal adhesion-targeting mechanism of pp125FAK. *J. Exp. Med. 182*, 1089−1099.
(26) Yano, H., Mazaki, Y., Kurokawa, K., Hanks, S. K., Matsuda, M., and Sabe, H. (2004) Roles played by a subset of integrin signaling molecules in cadherin-based cell-cell adhesion. *J. Cell Biol. 166*, 283−295.
(27) Liu, G., Guibao, C. D., and Zheng, J. (2002) Structural insight into the mechanisms of targeting and signaling of focal adhesion kinase. *Mol. Cell. Biol. 22*, 2751−2760.
(28) Gao, G., Prutzman, K. C., King, M. L., Scheswohl, D. M., DeRose, E. F., London, R. E., Schaller, M. D., and Campbell, S. L. (2004) NMR solution structure of the focal adhesion targeting domain of focal adhesion kinase in complex with a paxillin LD peptide: evidence for a two-site binding model. *J. Biol. Chem. 279*, 8441−8451.
(29) Arold, S. T., Hoellerer, M. K., and Noble, M. E. (2002) The structural basis of localization and signaling by the focal adhesion targeting domain. *Structure 10*, 319−327.
(30) Hayashi, I., Vuori, K., and Liddington, R. C. (2002) The focal adhesion targeting (FAT) region of focal adhesion kinase is a four-helix bundle that binds paxillin. *Nat. Struct. Biol. 9*, 101−106.
(31) Magis, A. T., Bailey, K. M., Kurenova, E. V., Hernandez Prada, J. A., Cance, W. G., and Ostrov, D. A. (2008) Crystallization of the focal adhesion kinase targeting (FAT) domain in a primitive orthorhombic space group. *Acta Crystallogr., Sect. F: Struct. Biol. Cryst. Commun. 64*, 564−566.
(32) Zhou, Z., Feng, H., and Bai, Y. (2006) Detection of a hidden folding intermediate in the focal adhesion target domain: Implications for its function and folding. *Proteins: Struct., Funct., Genet. 65*, 259−265.
(33) Bertolucci, C. M., Guibao, C. D., and Zheng, J. (2005) Structural features of the focal adhesion kinase-paxillin complex give insight into the dynamics of focal adhesion assembly. *Protein Sci. 14*, 644−652.
(34) Lulo, J., Yuzawa, S., and Schlessinger, J. (2009) Crystal structures of free and ligand-bound focal adhesion targeting domain of Pyk2. *Biochem. Biophys. Res. Commun. 383*, 347−352.
(35) Scheswohl, D. M., Harrell, J. R., Rajfur, Z., Gao, G., Campbell, S. L., and Schaller, M. D. (2014) Multiple paxillin binding sites regulate FAK function. *J. Mol. Signaling 3*, 1.
(36) Vanarotti, M. S., Miller, D. J., Guibao, C. D., Nourse, A., and Zheng, J. J. (2014) Structural and mechanistic insights into the interaction between Pyk2 and paxillin LD motifs. *J. Mol. Biol. 426*, 3985−4001.
(37) Lipsky, B. P., Beals, C. R., and Staunton, D. E. (1998) Leupaxin is a novel LIM domain protein that forms a complex with PYK2. *J. Biol. Chem. 273*, 11709−11713.
(38) Sahu, S. N., Nunez, S., Bai, G., and Gupta, A. (2007) Interaction of Pyk2 and PTP-PEST with leupaxin in prostate cancer cells. *Am. J. Physiol Cell Physiol 292*, C2288−C2296.
(39) Lorenz, S., Vakonakis, I., Lowe, E. D., Campbell, I. D., Noble, M. E., and Hoellerer, M. K. (2008) Structural analysis of the interactions between paxillin LD motifs and alpha-parvin. *Structure 16*, 1521−1531.
(40) Bos, P. D., Zhang, X. H., Nadal, C., Shu, W., Gomis, R. R., Nguyen, D. X., Minn, A. J., van de Vijver, M. J., Gerald, W. L., Foekens, J. A., and Massague, J. (2009) Genes that mediate breast cancer metastasis to the brain. *Nature 459*, 1005−1009.
(41) Neidhardt, F. C., Bloch, P. L., and Smith, D. F. (1974) Culture medium for enterobacteria. *J. Bacteriol. 119*, 736−747.
(42) Zhang, Z. M., Simmerman, J. A., Guibao, C. D., and Zheng, J. J. (2008) GIT1 paxillin-binding domain is a four-helix bundle, and it binds to both paxillin LD2 and LD4 motifs. *J. Biol. Chem. 283*, 18685−18693.
(43) Emsley, P., and Cowtan, K. (2004) Coot: model-building tools for molecular graphics. *Acta Crystallogr., Sect. D: Biol. Crystallogr. 60*, 2126−2132.
(44) Adams, P. D., Afonine, P. V., Bunkoczi, G., Chen, V. B., Davis, I. W., Echols, N., Headd, J. J., Hung, L. W., Kapral, G. J., Grosse-Kunstleve, R. W., McCoy, A. J., Moriarty, N. W., Oeffner, R., Read, R. J., Richardson, D. C., Richardson, J. S., Terwilliger, T. C., and Zwart, P. H. (2010) PHENIX: a comprehensive Python-based system for macromolecular structure solution. *Acta Crystallogr., Sect. D: Biol. Crystallogr. 66*, 213−221.
(45) Chen, V. B., Arendall, W. B., 3rd, Headd, J. J., Keedy, D. A., Immormino, R. M., Kapral, G. J., Murray, L. W., Richardson, J. S., and Richardson, D. C. (2010) MolProbity: all-atom structure validation for macromolecular crystallography. *Acta Crystallogr., Sect. D: Biol. Crystallogr. 66*, 12−21.
(46) DeLano, W. L. 2002. The PyMOL Molecular Graphics System. DeLano Scientific; San Carlos.
(47) Otwinowski, Z. M., and Minor, W. (1997) Processing of X-ray diffraction data collected in oscillation mode. *Methods Enzymol. 276*, 307−326.

DOI: 10.1021/acs.biochem.5b01274
Biochemistry 2016, 55, 1332−1345

(48) McCoy, A. J., Grosse-Kunstleve, R. W., Adams, P. D., Winn, M. D., Storoni, L. C., and Read, R. J. (2007) Phaser crystallographic software. *J. Appl. Crystallogr. 40*, 658−674.
(49) Kabsch, W. (2010) Xds. *Acta Crystallogr., Sect. D: Biol. Crystallogr. 66*, 125−132.
(50) Keller, R. 2004. The Computer Aided Resonance Assignment Tutorial. Verlag, Cantina, Switzerland.
(51) Farmer, B. T., 2nd, Constantine, K. L., Goldfarb, V., Friedrichs, M. S., Wittekind, M., Yanchunas, J., Jr., Robertson, J. G., and Mueller, L. (1996) Localizing the NADP+ binding site on the MurB enzyme by NMR. *Nat. Struct. Biol. 3*, 995−997.
(52) Garrett, D. S., Seok, Y. J., Peterkofsky, A., Clore, G. M., and Gronenborn, A. M. (1997) Identification by NMR of the binding surface for the histidine-containing phosphocarrier protein HPr on the N-terminal domain of enzyme I of the Escherichia coli phosphotransferase system. *Biochemistry 36*, 4393−4398.
(53) Grzesiek, S., Bax, A., Clore, G. M., Gronenborn, A. M., Hu, J. S., Kaufman, J., Palmer, I., Stahl, S. J., and Wingfield, P. T. (1996) The solution structure of HIV-1 Nef reveals an unexpected fold and permits delineation of the binding surface for the SH3 domain of Hck tyrosine protein kinase. *Nat. Struct. Biol. 3*, 340−345.
(54) Zrihan-Licht, S., Fu, Y., Settleman, J., Schinkmann, K., Shaw, L., Keydar, I., Avraham, S., and Avraham, H. (2000) RAFTK/Pyk2 tyrosine kinase mediates the association of p190 RhoGAP with RasGAP and is involved in breast cancer cell invasion. *Oncogene 19*, 1318−1328.
(55) Chen, P. W., and Kroog, G. S. (2010) Leupaxin is similar to paxillin in focal adhesion targeting and tyrosine phosphorylation but has distinct roles in cell adhesion and spreading. *Cell adhesion & migration 4*, 527−540.
(56) Thompson, J. D., Higgins, D. G., and Gibson, T. J. (1994) CLUSTAL W: improving the sensitivity of progressive multiple sequence alignment through sequence weighting, position-specific gap penalties and weight matrix choice. *Nucleic Acids Res. 22*, 4673−4680.
(57) Katsumi, A., Kiyoi, H., Abe, A., Tanizaki, R., Iwasaki, T., Kobayashi, M., Matsushita, T., Kaibuchi, K., Senga, T., Kojima, T., Kohno, T., Hamaguchi, M., and Naoe, T. (2011) FLT3/ ITD regulates leukaemia cell adhesion through alpha4beta1 integrin and Pyk2 signalling. *Eur. J. Haematol. 86*, 191−198.
(58) Sun, C. K., Ng, K. T., Lim, Z. X., Cheng, Q., Lo, C. M., Poon, R. T., Man, K., Wong, N., and Fan, S. T. (2011) Proline-rich tyrosine kinase 2 (Pyk2) promotes cell motility of hepatocellular carcinoma through induction of epithelial to mesenchymal transition. *PLoS One 6*, e18878.

DOI: 10.1021/acs.biochem.5b01274
Biochemistry 2016, 55, 1332−1345